C. R. Chimie 18 (2015) 277–282

Contents lists available at ScienceDirect

Comptes Rendus Chimie

www.sciencedirect.com

GeCat 2014: Advances and prospects in heterogeneous catalysis

CO_2 reforming of CH_4 over highly active and stable *y*RhNi*x*/NaY catalysts

Reformage du méthane par le dioxyde de carbone sur des catalyseurs y*RhNix/NaY actifs et stables*

Jane Estephane [a,*], Marc Ayoub [a], Khaled Safieh [a], Marie-Nour Kaydouh [a], Sandra Casale [b], Henri El Zakhem [a]

[a] *Department of Chemical Engineering, Faculty of Engineering, University of Balamand, PO Box 33, Tripoli, Lebanon*
[b] *Laboratoire de réactivité de surface, CNRS UMR 7197, Université Pierre-et-Marie-Curie, 4, place Jussieu, case courrier 178, 75252 Paris cedex 05, France*

ARTICLE INFO

Article history:
Received 23 May 2014
Accepted after revision 18 August 2014
Available online 7 February 2015

Keywords:
Dry reforming
Nickel
Rhodium
Syngas
Zeolite NaY

ABSTRACT

$Ni_{7.5}$/NaY catalysts were prepared using two different methods, the incipient wetness impregnation method and the "two-solvent" method. These catalysts were characterised by N_2 sorption, XRD, TEM and TPR. Their activity and stability in the dry reforming of methane were tested at atmospheric pressure under an equimolar mixture of methane and carbon dioxide. Three different Ni species, very small, spherical, and layers of nickel silicate were observed by TEM. The preparation by the two-solvent method led to a better dispersion of the active phase as well as to better activity and stability. These catalysts were promoted with small amounts (0.1 wt%) of rhodium. Rhodium facilitates the reducibility and greatly enhances catalytic activity. A complete conversion (100%) for CH_4 and CO_2 over the Rh promoted catalyst is achieved at 584 °C and 559 °C respectively, while for the non-promoted Ni7.5/NaY catalyst, only a 60% conversion rate for CH_4 and CO_2 is reached at the same temperatures.

Mots clés :
Reformage à sec
Nickel
Rhodium
Syngas
Zéolithe NaY

RÉSUMÉ

Des catalyseurs $Ni_{7,5}$/NaY ont étés préparés par imprégnation à sec et par la méthode à deux solvants. Ces catalyseurs ont étés caractérisés par physisorption d'azote, DRX, MET et RTP. Leur activité et stabilité ont été testées dans le reformage à sec du méthane sous pression atmosphérique et un mélange équimolaire de méthane et de dioxyde de carbone. Trois différentes espèces de nickel, sphériques, de très petites tailles ou des feuillets de silicate de nickel ont été détectées par MET. La méthode à deux solvants permet de mieux disperser la phase active et d'augmenter l'activité catalytique. Ces catalyseurs ont été promus par un faible pourcentage de rhodium. Ce dernier facilite la réduction et augmente significativement l'activité et la stabilité. Une conversion totale (100 %) du méthane et du

* Corresponding author.
E-mail addresses: jane.estephane@balamand.edu.lb (J. Estephane), marc.ayoub@std.balamand.edu.lb (M. Ayoub), khaled.safieh@std.balamand.edu.lb (K. Safieh), marie.kaydouh@std.balamand.edu.lb (M.-N. Kaydouh), Sandra.casale@upmc.fr (S. Casale), henri.elzakhem@balamand.edu.lb (H.E. Zakhem).

http://dx.doi.org/10.1016/j.crci.2014.08.007
1631-0748/

dioxyde de carbone a été obtenue à 584 °C et 559 °C respectivement, sur le catalyseur promu par du Rh, tandis que sur le catalyseur $Ni_{7,5}$/NaY non promu, la conversion du CH_4 et du CO_2 n'est que de 60 % aux mêmes températures.

1. Introduction

With the increasing demand for energy nowadays and the depletion of conventional resources, such as crude oil, the need for new energy sources has gained great importance. Natural gas, with its large proved reserves, plays an increasing energetic role and can contribute to supply the enormous demand for energy [1].

In order to transform natural gas, which contains mostly methane, into valuable products (hydrogen and syngas), the dry reforming of CH_4 is gaining increasing attention worldwide [2,3]. This process offers advantages over the partial oxidation and steam reforming, such as the conversion of the two cheapest and most abundant greenhouse gases (CO_2 and CH_4) into useful syngas [4], as well as the production of syngas with an H_2/CO ratio of 1:1 [5]. The synthesized gas produced is used in various industrial processes, such as methanol and Fischer–Tropsch syntheses [6,7].

Coke deposition and sintering are the main drawbacks for dry reforming that lead to the rapid deactivation of the catalysts. Supported noble metals, such as Pt, Ru and Rh, are known to have high activity, stability and resistance to coke formation at high temperatures [8,9], especially when Rh is used [10,11]. However, their high cost and limited availability make them a non-reliable choice. It has been shown that adding a small amount of noble metals (Pt, Pd, Ru and Rh) to Ni catalysts resulted in interesting observations and a significant enhancement in catalytic activity and stability [12,13].

Besides the metal, the catalyst support plays an important role in the activity of the catalysts. Zeolites form attractive supports for dry reforming of methane, since they have a well-defined structure, high thermal stabilities, and high surface areas [14–16]. It is also known that zeolite supports offer high metal dispersion with low support metal interactions. These properties, combined together, make zeolites attractive supports that enhance catalytic activity and selectivity in the CO_2 reforming of CH_4 [14]. The nature of the zeolite support has a significant impact on the performance of the catalyst in the dry reforming of methane [13,17–19]. NaY zeolites with a FAU framework type have high potential properties, such as the microporous structure and a high affinity for CO_2 adsorption, which highly improve the activity as well as the selectivity of the catalysts in reforming reactions.

Furthermore, the method of preparation influences the catalytic activity by increasing the dispersion of the active phase. The two-solvent methods [20] were used to highly disperse, inside the porosity of SBA-15, different metal oxide species [21–23].

No previous work reported the use of the "two-solvent" impregnation method for the preparation of zeolite catalysts. In this contribution, the effect of the preparation method ("two-solvent" vs. the incipient wetness impregnation method) on the overall performance of the catalysts in DRM is investigated. The effect of combining the high coke-resistance of noble metal Rh and the good activity, availability and reasonable price of non-noble metal Ni is studied. On this basis, in the present work, activity, selectivity and stability results concerning the dry reforming of methane by NaY-supported Ni catalysts (Ni_x/NaY) having a 7.5 wt% Ni loading ($x = 7.5$) are reported. A small amount (0.1 wt%) of Rh was added to the non-promoted Ni7.5S/NaY catalyst that showed the best catalytic performance in CO_2 dry reforming. The goal is to obtain an enhancement in catalytic performance.

2. Experimental

NaY-supported monometallic nickel catalysts were prepared by incipient wetness impregnation method [24], where an aqueous solution of nickel (II) nitrate hexahydrate (99.99%; Sigma–Aldrich) was added to NaY zeolite (supplied by Sigma–Aldrich) or by the two-solvent impregnation method [20] to obtain the desired load of Ni (7.5 wt%).

These monometallic catalysts were left to dry at room temperature for 24 h, and then calcined in a muffle furnace for 5 h at 450 °C at a heating rate of 0.5 °C/min. The prepared samples were denoted as NixI/NaY and NixS/NaY (where $x = 7.5$ wt%, I = incipient wetness impregnation method, S = two-solvent impregnation method).

For the preparation of the rhodium–nickel catalyst, a solution of Rh (III) nitrate hydrate (Sigma–Aldrich) was added to the previously prepared and calcined monometallic Ni7.5S/NaY catalyst to obtain a loading of 0.1 wt% of Rh. The rhodium–nickel catalyst was calcined again under the same conditions as those described above. The final sample was identified as 0.1RhNi7.5S/NaY.

The Brunauer–Emmett–Teller (BET) surface area of the catalysts was determined in a Thermo-Electron QSurf M1 apparatus using the BET method. Prior to analysis, the calcined catalysts were treated under a helium flow at 120 °C for 30 min. The temperature-programmed reduction (TPR) experiments were conducted using an AutoChem 2920 (Micromeritics) apparatus to determine the reducible species and the corresponding reduction temperatures. The catalyst powder (40 mg) was placed in a U-tube quartz reactor. A 5-volume% of H_2/Ar was fed over the calcined catalyst powder under atmospheric pressure, at a continuous flow rate of 20 mL/min. The temperature was increased from room temperature to 1000 °C. During TPR analysis, water was trapped in a bath of ice and salt. The variation of the amount of H_2 consumed as a function of temperature is recorded by means of the thermal

conductivity detector (TCD). X-ray diffraction (XRD) experiments were carried out on a Bruker D8 diffractometer using Cu Kα radiation (λ = 1.5405 nm) and operating at 40 kV and 30 mA. The diffraction intensities were measured over an angular range of $5^\circ < 2\Theta < 80^\circ$ for all the samples with a step size of $2\Theta = 0.02^\circ$. High-Resolution Transmission Electron Microscopy (HR-TEM) experiments were conducted on a JEOL JEM-200 electron microscope operating at 200 keV (LaB_6 gun) equipped with an energy dispersive X-ray spectroscopy (EDXS) and selected area electron diffraction (SAED). A small amount of sample was suspended in ethanol and dispersed over a Cu grid coated with a 10-nm carbon membrane. The average particle size of the active phase was determined using the Comptage de particules-volume 2 software.

The catalytic activity determination was carried out using 40 mg of catalyst under atmospheric pressure. For all the experiments, the reactants mixture consisting of CH_4 and CO_2 (molar ratio $CH_4/CO_2 = 1:1$) was fed at 200 °C with a GHSV of 193,500 $mL \cdot g^{-1} \cdot h^{-1}$, then, the reaction temperature was increased from 200 °C up to 800 °C at a heating rate of 5 °C·min^{-1}. For the stability measurements, the reactor was cooled down to 500 °C and maintained at this temperature for 12 h. Prior to the catalytic tests, each catalyst was reduced in situ at 650 °C with 5 vol% H_2/Ar for 2 h. The reactants and products were analyzed online by a Micro-GC Inficon equipped with a thermal conductivity detector (TCD) and two columns (Molecular Sieve 5 Å and Plot U) used for a complete separation of hydrogen, methane, carbon monoxide, and carbon dioxide.

The conversions of CH_4 and CO_2 (X_{CH_4} and X_{CO_2}) were calculated as follows:

$$X_{CH_4} = \frac{[CH_4]_{in} - [CH_4]_{out}}{[CH_4]_{in}} \times 100$$

$$X_{CO_2} = \frac{[CO_2]_{in} - [CO_2]_{out}}{[CO_2]_{in}} \times 100$$

where $[CH_4]_{in}$, $[CO_2]_{in}$ are the molar flow rates of the introduced reactants, and $[CH_4]_{out}$, $[CO_2]_{out}$ are the molar flow rates of the corresponding compositions in the effluents.

3. Results and discussion

The BET surface area of the support NaY and of the various impregnated catalysts are summarized in Table 1. The NaY zeolite samples presented the highest value of surface area. As expected, the introduction of nickel into the framework of NaY zeolite reduced the BET surface from 887 to 608 m^2/g with the incipient wetness impregnation technique and from 889 to 704 m^2/g with the two-solvent method.

Table 1
Surface area of the NaY zeolite and of the different catalysts.

Catalyst	BET surface area (m^2/g)
NaY	940
$Ni_{7.5}I/NaY$	612
$Ni_{7.5}S/NaY$	702
$0.1RhNi_{7.5}S/NaY$	705

The XRD patterns of the NaY, Ni7.5I/NaY, Ni7.5S/NaY and 0.1RhNi7.5S/NaY catalysts are reported in Fig. 1. The XRD profile of the NaY presents diffraction peaks (*) characteristic of zeolite Y [25,26]. The diffraction patterns of the Ni7.5I/NaY and Ni7.5S/NaY catalysts show a similar crystallinity to that of the NaY zeolite. This indicates that the zeolite structure is preserved in the two solids [27]. However, the small decrease in the intensity of the diffraction peaks indicates that the zeolite crystallinity decreased upon Ni incorporation [27,28]. Moreover, no NiO diffraction peaks are observed. This is due to the presence of highly dispersed and/or amorphous Ni based species on the surface of the zeolite. The addition of 0.1 wt% rhodium did not affect the diffraction profile. The diffraction peaks corresponding to the different rhodium

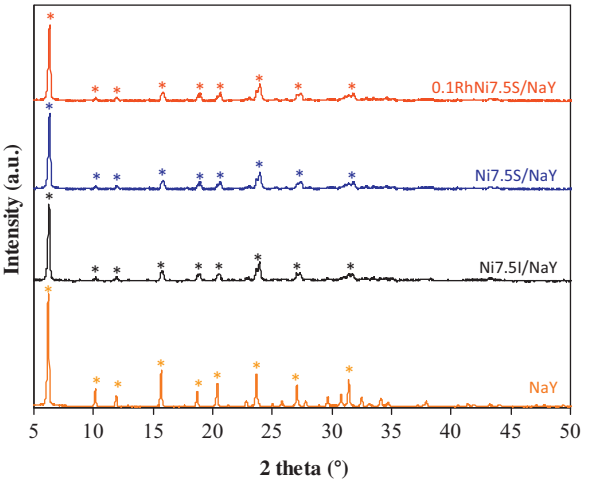

Fig. 1. (Color online.) XRD patterns of NaY, Ni7.5I/NaY, Ni7.5S/NaY and 0.1RhNi7.5S/NaY calcined catalysts.

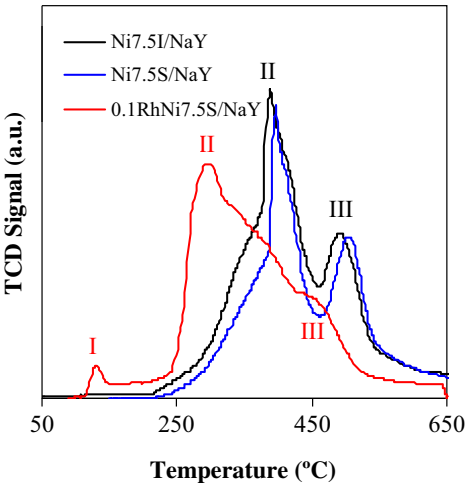

Fig. 2. (Color online.) TPR Profiles for Ni7.5I/NaY, Ni7.5S/NaY and 0.1RhNi7.5S/NaY catalysts.

oxide species (RhO, Rh_2O_3, Rh_2O...) are absent. This might be due to the low rhodium content in the solid in addition to the dispersion of the species on the surface of the support.

Fig. 2 shows the temperature-programmed reduction profiles of the calcined Ni7.5I/NaY, Ni7.5S/NaY and 0.1RhNi7.5S/NaY catalysts. It is to note that the TPR profile of the support does not show any reduction phenomena in the considered temperature range (result not shown). The TPR profiles of the Ni7.5I/NaY and Ni7.5S/NaY solids follow similar trends. In fact, two reduction zones are identified between 250 and 450 °C (peak II) and between 450 and 625 °C (peak III), respectively. These reduction peaks are attributed to the reduction of NiO species with low interaction with the support [29] and present at the level of the supercage and/or sodalite cavities [30]. In the literature [31], it is reported that a reduction peak at higher temperature (~800 °C) is observed for similar solids, which was attributed to the reduction of Ni (II) species having a strong interaction with the support [32] and/or present in the hexagonal prisms [31]. These species are minor in our case, as the experimental H_2 consumptions (peaks II and III) are approximately equal to the theoretical ones calculated for the reduction of NiO into metallic Ni. The TPR profile of the 0.1RhNi7.5S/NaY solid exhibits a reduction peak at 132 °C (peak I). In addition, the NiO reduction peaks for this solid (peaks II and III) are obtained at lower temperatures relatively to the rhodium-free catalysts' profiles. Peak I is unambiguously attributed to rhodium oxide species [33]. The left shift in the temperatures of peaks II and III indicates that the promotion of the solid with rhodium makes the reduction of nickel oxide species dispersed over the surface easier. It is known that the presence of reduced rhodium facilitates the "spill-over"

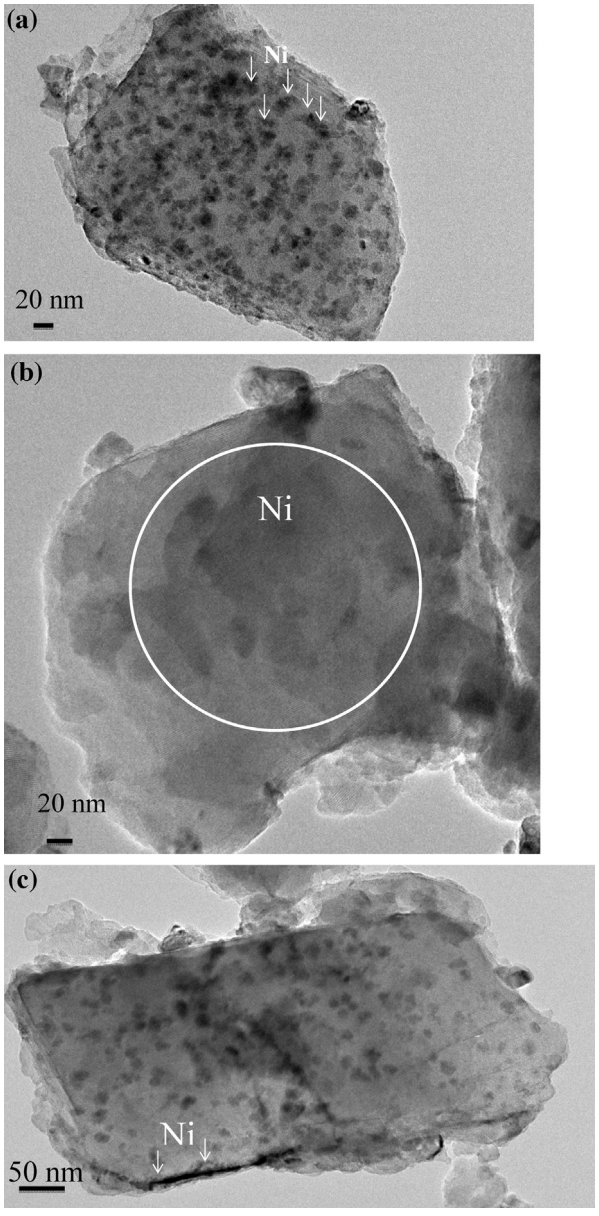

Fig. 3. TEM images of (a and b) Ni7.5I/NaY and (c) Ni7.5S/NaY catalysts.

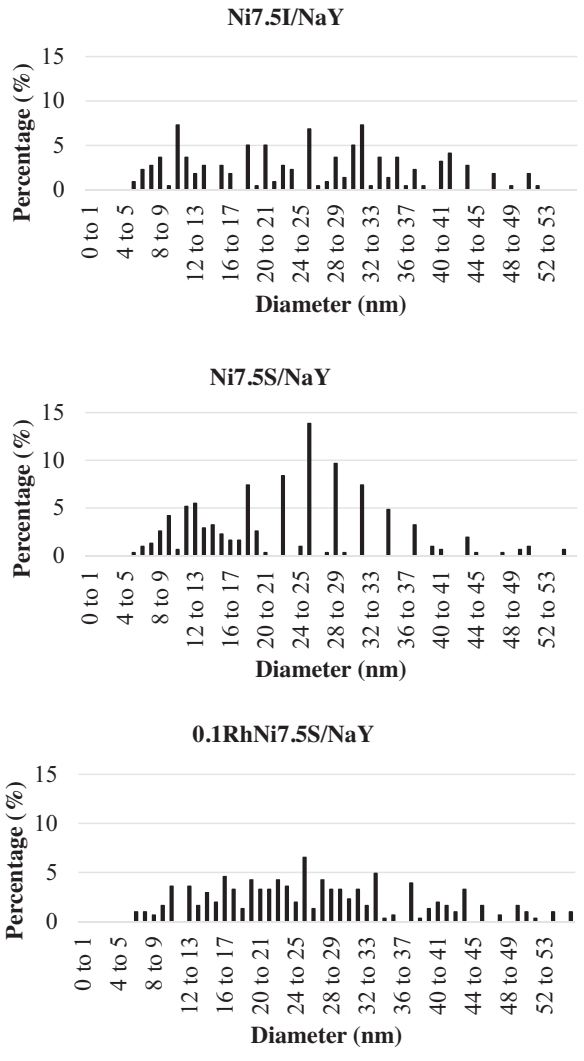

Fig. 4. Particle size distribution of the different catalysts.

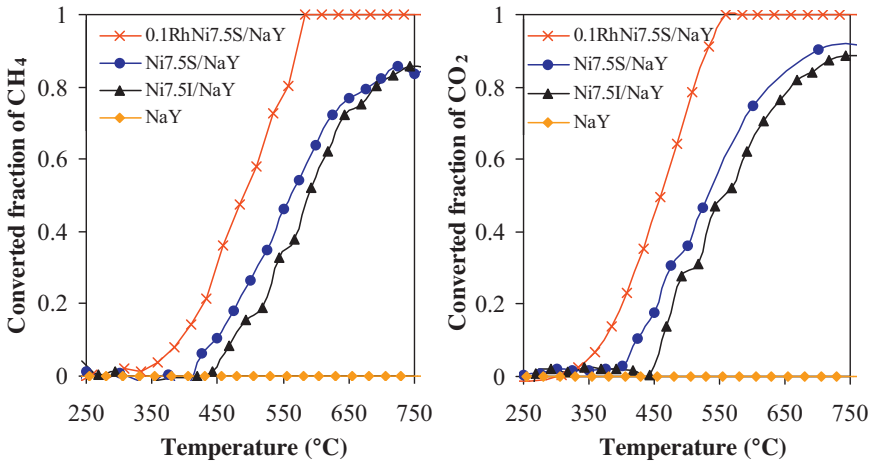

Fig. 5. (Color online.) CH_4 and CO_2 conversions over NaY, Ni7.5I/NaY, Ni7.5S/NaY and 0.1RhNi7.5S/NaY catalysts (molar ratio of $CH_4/CO_2 = 1$ and GHSV = 193,500 mL·g^{-1}·h^{-1}).

of the hydrogen molecules generating more reactive hydrogen radicals.

Fig. 3 shows that nickel is present in three different forms on the catalysts: spherical particles (Fig. 3a), very small particles detected by EDS but hard to detect on TEM micrographs (Fig. 3b), and layers of nickel silicate (Fig. 3c). No clear difference between the catalysts can be seen on TEM micrographs. However, particle size distributions (Fig. 4a–c) determined from statistical counting of nickel particles indicates smaller particles for the Ni7.5S/NaY catalyst. The average particle sizes are 23.8, 25.5, and 26.5 nm for Ni7.5S/NaY, Ni7.5I/NaY and 0.1RhNi7.5S/NaY respectively. For the same Ni/Si ratio (0.22) in the Ni7.5S/NaY and Ni7.5I/NaY catalysts, Na/Ni ratio decreases from 0.4 to 0.32, respectively. This indicates a better exchange of nickel leading to a better dispersion when using the two-solvent method.

Fig. 5 shows the CH_4 and CO_2 conversions over the different calcined solids. Over the 250–750 °C temperature range, the support is inactive in the considered reaction. The addition of 7.5 wt% of nickel by the impregnation method allowed the conversion of 50% of CH_4 at 590 °C and of 50% of CO_2 at 550 °C. At 750 °C, the conversions of CH_4 and CO_2 reached 87%. For the Ni7.5S/NaY solid, the activity in the DRM reaction is slightly enhanced. In fact, the temperatures of 50% conversion ($T_{50\%}$) for both reactant gases are decreased by ~20 °C. A similar conversion of ~87% is obtained at 750 °C. This result indicates that the Ni catalytic sites in the catalyst prepared by the two-solvent method are more active in the low-temperature range (reaction under catalytic control), while this improvement is less obvious in the high-temperature range (reaction under thermal control). The promotion of the Ni7.5S/NaY catalyst with 0.1 wt% rhodium showed a marked increase in the conversion of both gases over the whole temperature range. The $T_{50\%}$ for CH_4 and CO_2 are 487 °C and 459 °C, respectively, while complete conversion (100%) for CH_4 and CO_2 is achieved at 584 °C and 559 °C. This is in agreement with the TPR results that show that the addition of Rh improved the redox properties of the solid, making it more catalytically active in the DRM reaction. It is noticed that H_2/CO ratio is less than 1 in the 250–600 °C range. This is due to the occurrence of secondary reactions such as the reverse water–gas shift reaction (RWGS) that consumes CO_2 (CO_2 conversion higher than CH_4 conversion in this temperature range in Fig. 5) and H_2 to form CO and H_2O. The H_2/CO ratio increases to ~1 at higher temperatures, at which the RWGS reaction is less favored.

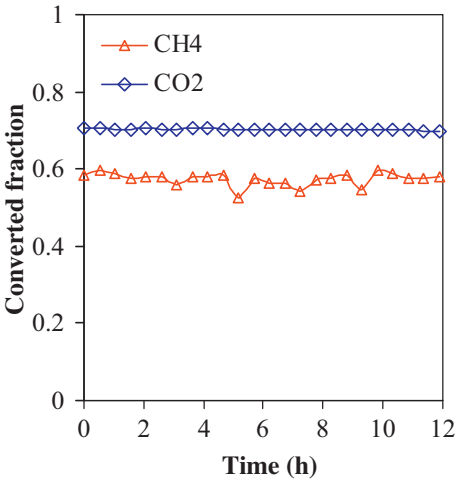

Fig. 6. (Color online.) CH_4 conversion and CO_2 conversion versus time-on-stream (TOS) over 0.1RhNi7.5S/NaY (500 °C, GHSV = 193,500 mL·g^{-1}·h^{-1}, 12 TOS).

Fig. 6 represents the results of an aging test in which the 0.1RhNi7.5S/NaY was kept on stream for 12 h at 500 °C. It is observed that the catalytic activity is unaltered over the test period, indicating that the catalyst is stable and is promising to be considered for industrial applications. The H_2/CO ratio remained unchanged during the test, thus, no side reactions are favored on the working catalyst.

4. Conclusion

A high dispersion of nickel oxides on NaY was obtained on the different catalysts prepared. The two-solvent

method enhanced the catalytic activity in the dry reforming of methane. The promotion with rhodium enhanced the redox properties of the Ni/NaY solid. This is beneficial for the DRM reaction as it occurs at relatively low temperatures. Finally, it was found that the 0.1RhNi7.5S/NaY catalyst exhibited the best catalytic performance. This catalyst is highly active (both for CH_4 and for CO_2 conversions), stable, and can be envisaged as a candidate for industrial applications.

Acknowledgments

Authors would like to thank Dr. Antoine El Samarani, Dr. Nissrine El Hassan and Miss Wadad Daaboul for their precious support.

References

[1] C.H. Bartholomew, R.J. Farrauto, Fundamentals of industrial catalytic processes, Wiley, New York, 2006.
[2] J.Z. Luo, Z.L. Yu, C.F. Ng, C.T. Au, J. Catal. 194 (2000) 198.
[3] S. Tang, L. Ji, H.C. Zeng, K.L. Tan, K. Li, J. Catal. 194 (2000) 424.
[4] B. Bachiller-Baeza, C. Mateos-Pedrero, M. Soria, A. Guerrero-Ruiz, U. Rodemerck, I. Rodríguez-Ramos, Appl Catal. B 129 (2013) 450.
[5] A.M. Gadalla, B. Bower, Chem. Eng. Sci. 43 (1988) 3049.
[6] P. Gangadharan, K.C. Kanchi, H.H. Lou, Chem. Eng. Res. Des. 90 (2012) 1956.
[7] A. Shamsi, ACS Petroleum Preprints 45 (2000) 690.
[8] M. García-Diéguez, I.S. Pieta, M.C. Herrera, M.A. Larrubia, L.J. Alemany, J. Catal. 270 (2010) 136.
[9] C. Yang-guang, K. Tomishige, K. Yokoyama, K. Fujimoto, Appl. Catal. A 165 (1997) 335.
[10] R.N. Bhat, W.M.H. Sachtler, Appl. Catal. A 150 (1997) 279.
[11] W.K. Józwiak, M. Nowosielska, J. Rynkowski, Appl. Catal. A 280 (2005) 233.
[12] Y.H. Hu, E. Ruckenstein, Adv. Catal. 48 (2004) 297.
[13] A.N. Pinheiro, A. Valentini, J.M. Sasaki, A.C. Oliveira, Appl. Catal. A 355 (2009) 156.
[14] B. Pavelec, S. Damyanova, K. Arishtirova, J.L. Fierro, L. Petrov, Appl. Catal. A 30 (2007) 188.
[15] J. Zhang, H. Wang, A.K. Dalai, J. Catal. 249 (2007) 300.
[16] W. Nimwattanakul, A. Luengnaruemitchai, S. Jitkarnka, Int. J. Hydrogen Energy 31 (2006) 93–100.
[17] P. Frontera, A. Aloise, A. Macario, P.L. Antonucci, F. Crea, G. Giordano, J.B. Nagy, Top. Catal. 53 (2010) 265.
[18] U.L. Portugal, C.M.P. Marques, E.C.C. Araujo, E.V. Morales, M.V. Giotto, J.M.C. Bueno, Appl. Catal. A: Gen. 193 (2000) 173.
[19] C. Crisafulli, S. Scirè, S. Minicò, L. Solarino, Appl. Catal. A: Gen. 225 (2002) 1.
[20] M. Imperor-Clerc, D. Bazin, M.D. Appay, P. Beaunier, A. Davidson, Chem. Mater. 16 (2004) 1813.
[21] F. Boubekr, A. Davidson, S. Casale, P. Massiani, Microp. Mesopor. Mater. 141 (2011) 157.
[22] J. Taghavimoghaddam, G.P. Knowles, A.L. Chaffee, Top. Catal. 55 (2012) 571.
[23] K. Jabbour, N. El Hassan, S. Casale, J. Estephane, H. El Zakhem, Int. J. Hydrogen Energy 39 (2014) 7780.
[24] U. Izquierdo, V.L. Barrio, J. Requies, J.F. Cambra, M.B. Güemez, P.L. Arias, Int. J. Hydrogen Energy 38 (2013) 7623.
[25] L. Guczi, D. Bazin, I. Kovacs, L. Borko, Z. Schay, J. Lynch, P. Parent, C. Lafon, G. Stefler, Z. Koppany, I. Sajo, Topics Catal. 20 (2002) 129.
[26] D. Ginter, Zeolite Y synthesis, in: H. Robson (Ed.), Verified Syntheses of Zeolitic Materials, 2nd ed., Elsevier, Amsterdam, 2001.
[27] P. Khemthong, W. Klysubun, S. Prayoonpokarach, J. Wittayakun, Mater. Chem. Phys. 121 (2010) 131.
[28] D. Kiessling, K. Hagenan, G. Wendt, A. Barth, R. Schoellner, React. Kinet. Catal. Lett. 39 (1989) 89.
[29] A. Luengnaruemitchai, A. Kaengsilalai, Chem. Eng. J. 144 (2008) 96.
[30] M. Afzal, G. Yasmeen, M. Saleem, J. Afzal, J. Therm. Anal. Cal. 62 (2000) 277.
[31] J.S. Feeley, W.M.H. Sachtler, Catal. Lett. 9 (1991) 377.
[32] A.M. Diskin, R.H. Cunningham, R.M. Ormerod, Catal. Today 46 (1998) 147.
[33] M. Boutros, F. Launay, A. Nowicki, T. Onfroy, V. Herledan-Semmer, A. Roucoux, A. Gédéon, J. Mol. Catal. A: Chem. 259 (2006) 91.